International Journal for Housing Science and Its Applications
Publish August 10, 2025. Volume 46, Issue 4 Pages 4642-4649

https://doi.org/10.70517/ijhsa464307

Quantitative analysis of endometrial tolerance ultrasound images in the framework of intelligent image processing

Yun Wang[1,*] and Yabiao Zeng[2]
[1] Ultrasound Department, Hunan Maternal and Child Health Hospital, Changsha, Hunan, 123456, China
[2] General Surgery Department, Changsha Hospital of Traditional Chinese Medicine, Changsha, Hunan, 123456, China
Corresponding authors: (e-mail: Mier0628@163.com).

Abstract Endometrial tolerance is one of the key factors for pregnancy success, yet traditional assessment methods such as endometrial thickness often do not fully reflect the true state of the endometrium. With the continuous advancement of imaging technology, ultrasound imaging, especially the combination of three-dimensional ultrasound and multimodal ultrasound, provides a new technological tool for assessing endometrial tolerance. In this study, endometrial tolerance was quantified using color Doppler three-dimensional ultrasound, which was aimed at assessing its predictive value for IVF-ET pregnancy outcome. One hundred and thirteen female patients proposed for assisted reproduction were selected for the study and divided into case and control groups and endometrial morphology, thickness, volume and hemodynamic parameters were collected. The results showed that the difference in endometrial thickness between the PCOS group and the control group was not statistically significant ($P>0.05$), but the endometrial elastic modulus values were significantly higher ($P<0.05$). In multimodal ultrasonography scores, endometrial thickness score, VFI index score and total multimodal ultrasonography score were significantly lower in the case group than in the control group ($P<0.05$). In addition, there was a significant positive correlation between endometrial blood flow VI, FI and VFI and VEGF mRNA expression level (r 0.744, 0.522, 0.435, respectively, $P<0.01$). These results suggest that 3D ultrasound combined with hemodynamic parameters can effectively reflect endometrial tolerance and provide a new assessment method for pregnancy prediction in IVF-ET.

Index Terms Endometrial tolerance, color Doppler ultrasound, three-dimensional ultrasound, VEGF mRNA, IVF-ET, hemodynamics

I. Introduction

Endometrial tolerance (ER) refers to the ability of the endometrium to allow embryo localization, adhesion, implantation and implantation during the endometrial “window period”, and is an important clinical indicator of the ability of the uterus to accommodate embryos [1]. High-quality embryos, good endometrial tolerance, and interaction between the embryo and the maternal endometrium are the key factors for a successful pregnancy, and a decrease in endometrial tolerance may increase the risk of empty sacs and fetal abruption, resulting in failure of embryo implantation, spontaneous abortion, and other adverse pregnancy outcomes [2]-[4]. According to relevant statistics, implantation failure occurs in about 1/3 of women due to poor embryo quality, and in 2/3 of women due to defective endometrial tolerance and synchronization between embryo and endometrium [5], [6]. In recent years, the detection and evaluation of endometrial tolerance has gradually become a hot research topic in clinical reproductive assisted conception.

Influenced by hormone levels, uterine structure and other factors, vaginal ultrasonography is often used to monitor endometrial thickness, endometrial and subendometrial blood flow information and other indicators for tolerance assessment, and then guide pregnancy, which is of high clinical utility [7]-[9]. However, the current ultrasound assessment relies on the experience of physicians, and due to the subjective influence, there are differences in the judgment of different physicians, and the quantitative assessment is based on a few parameters such as endometrial thickness, which lacks comprehensiveness, resulting in differences in the appropriateness of the timing of implantation of the embryo and lowering the clinical pregnancy rate [10]-[12]. In addition, dynamic information such as subendometrial blood flow cannot be captured by physicians, highlighting the dynamic flaws of ultrasound assessment [13]. Intelligent processing techniques bring advantages to break the ice in ultrasound image analysis. For example, deep learning can adapt the temporal sequence of bleeding to capture and enhance images [14], [15]. Three-dimensional U-Net segmentation technique enables automatic assessment by segmenting the endothelium [16].

In this study, a new assessment model of endometrial tolerance was proposed based on three-dimensional ultrasound imaging technology, combined with conventional endometrial thickness measurement and hemodynamic parameters. Female patients with plans to undergo assisted reproduction were selected for the study, and data on endometrial thickness, volume, and hemodynamic parameters were obtained by color Doppler ultrasound and three-dimensional energy Doppler technology, and the relationship between these parameters and pregnancy outcome was analyzed. The correlation between endothelial blood flow and VEGF expression levels was also explored and combined with multimodal ultrasound scoring for assisted judgment, with the aim of providing a more reliable assessment tool for assisted reproduction. The core of this study is to further improve the diagnostic criteria for endometrial tolerance through multifaceted imaging assessment, and to provide more clinical references.

II. Information and methods

II. A. General information

A total of 113 patients who planned to undergo assisted reproduction in a maternal and child health hospital in Shanghai from June 2023 to October 2024 were selected and all received transvaginal 3D ultrasound detection before pregnancy, and were divided into case group (n=166) and control group (n=198) according to whether they were clinically pregnant. Inclusion criteria: (1) Female patients aged 24~49 years old who intend to undergo assisted reproductive technology; (2) Menstrual cycle 1~47d; (3) No serious heart, liver, kidney and other important organ diseases; (4) No reproductive system tumor diseases, endometriosis and other diseases that affect the receptivity of the endometrium; (5) No endocrine disorders, immune system diseases and other diseases that affect fertility. Exclusion criteria: (1) Patients with genital tract inflammation, hemorrhagic disorders and cervical adhesions in the uterine cavity; (2) Polyps, submucosal fibroids, endometriosis and uterine malformations in the endometrium; (3) Patients with abnormal thyroid function; (4) Patients with reduced ovarian reserve, early-onset ovarian insufficiency and premature ovarian failure; (5) Immune infertility; (6) Those with mental illness.

II. B. Research methodology

Color Doppler ultrasound (Instrument model: GE Volu-son E10 and 3D energy Doppler ultrasound imaging with a transvaginal 3D volumetric probe was used. Parameters such as probe frequency (between 6 and 10 MHz), pulse frequency (0.6 kHz) sweep angle (180°), and color quality were set to ensure that clear endometrial images were obtained. The patient empties the bladder and maintains the cystotomy position, and ensures that the probe is sterilized cleanly, and a disposable ultrasound isolation sleeve is applied to the tip of the probe, and the vaginal ultrasound probe is slowly inserted into the patient's vagina up to the posterior fornix to observe the uterus, adnexa and pelvis, and to record the morphology and thickness of the endometrium; the 3D imaging mode is activated to obtain the three-dimensional reconstruction of endometrial images. All acquired ultrasound images and data were recorded and stored in real time for subsequent analysis.

II. C. Ultrasound indicators

The following indicators were collected: endometrial morphology, endometrial thickness, endometrial volume, endometrial and subendometrial RI, PI, FI, VI, VFI.

Endometrial morphology: endometrial morphology was classified into three types: type A endometrium, which showed the “three lines sign”, consisting of high echoes in the middle and low echoes on both sides; type B endometrium, which was homogeneous and moderately echogenic, with intermittent strong echoes in the center of the uterine cavity; and type C endometrium, which was homogeneous and strong echoes, with no echoes in the center of the uterine cavity and disappearance of the “three lines sign”. Type C endometrium is homogeneous and strong echogenicity, with no midline echogenicity and disappearance of the “three-line sign”.

Endometrial thickness: The distance between the strong echoes of the endometrium and the myometrial junction of the anterior and posterior walls of the uterine cavity was measured at a distance of 2 centimeters from the fundus of the uterus in the sagittal plane of the uterus, which could clearly show the morphology of the endometrium from the endocervical os to the fundus of the uterus.

Endometrial volume: Using three-dimensional volumetric imaging superimposed on a two-dimensional image, the endometrial image is captured at a moderate scanning speed, and the endometrial volume is calculated using the instrument's specialized software.

Endothelial and subendothelial hemodynamic parameters: The subendothelial and endothelial blood flow is visualized by color Doppler ultrasound, and the sampling frame is placed at the most obvious point of the blood flow signal and the blood flow spectrum is measured, and the corresponding hemodynamic values including RI and PI are measured after the appearance of three stable waveforms, and the 3-D energy Doppler mode is activated, and

the area of interest is scanned at a moderate scanning speed, and the FI, VI, and VF are calculated with the software of the instrument. FI, VI, and VFI.

II. D.Evaluation of ultrasound image features

II. D. 1) Feature extraction and normalization

The above mentioned platform is used to extract the image histological features. The raw features include first order, shape and texture features extracted from the original image. In addition, transformed images are generated using eight filters such as exponential, gradient, local binary mode, logarithmic, square, square root, wavelet and Gaussian Laplacian [17]. In addition to shape features, first order features and texture features can be extracted from the transformed images. Texture features are used to describe the heterogeneity of the tumor and include gray scale covariance matrix [18], gray scale correlation matrix, gray scale tour matrix, radian region size matrix, and neighborhood gray scale difference matrix. z-score normalization is used to reduce the potential effects associated with various parameters.

$$Z = (x - \mu) / \sigma \tag{1}$$

where z is the standardized score, x is the original value, μ is the mean, and σ is the standard deviation.

II. D. 2) Feature selection and model construction

In order to reduce the computational complexity and improve the classification accuracy, nine feature selection methods: variance threshold filter, optimal feature filter (number), optimal feature filter (percentage), filter according to significance, select according to model, iterative feature filter, stable feature filter, minimum redundancy maximum relevance and fast relevance filtering algorithms are used to select the optimal features; and seven classifiers: k-nearest neighbor, support Vector Machine, Logistic Regression, Decision Tree, Gradient Boosting Tree, Random Forest and Extreme Gradient Boosting algorithms to construct the model. Nine feature selection methods and seven classifiers were combined to form a total of 63 combinations. The combination with the best predictive efficacy is taken as the final result.

II. D. 3) Model Evaluation and Validation

The predictive efficacy of the model was further validated by internal validation set and 10-fold cross validation set. Subject operating characteristic curves were plotted and area under the curve, sensitivity, specificity and accuracy were calculated. The fitted curves were used to assess the agreement between the predictive model and the actual situation.DCA was used to assess the clinical value of the model based on calculating the NB at different threshold probabilities.

II. E. Statistical analysis

R 4.1.3 and IBM SPSS 26.0 software were used. Count information was expressed as n (%). Measurement information was confirmed to be skewed distribution after Kolmogorov-Smirnov test and was expressed as M(Q1,Q3). Categorical variables were analyzed using the chi-square test, and continuous variables were analyzed using the Mann-Whitney U test.Differences were considered statistically significant at $p<0.05$.

III. Results and analysis

III. A. Comparison of basic information between the PCOS group and the control group

The results of the comparison of the baseline data between the case group (PCOS) and the control group are shown in Table 1.There was no statistically significant difference between the PCOS group and the control group in terms of age, BMI, diameter of mature follicles, and hormones ($P > 0.05$).

Table 1: The case group was compared with the basic data of the control group($\bar{x} \pm s$)

Group	Age	BMI	Mature follicle diameter (mm)	Progesterone (ng/L)	Estradiol (μg /L)
PCOS group	31.28±3.57	29.13±0.97	20.65±1.73	9.22±0.91	361.17±28.19
Control group	30.19±2.47	24.35±1.18	18.59±1.54	9.81±1.18	365.63±23.58
T value	3.17	2.87	2.29	0.09	0.05
P value	0.22	0.17	>0.05	0.91	>0.05

III. B. Endometrial thickness and elastic modulus value test in both groups

Figures 1 to 4 show the results of the analysis of the PCOS group and the control group in terms of endothelial thickness and elasticity values collected in this study. The data were normally distributed. The endometrial thickness

and elasticity modulus values of the subjects ranged from 0.85 to 1.75 mm and 13.54 to 49 kPa, respectively, and the difference in overall endometrial thickness between the PCOS group and the control group was not statistically significant (P > 0.05), while the difference in endometrial elasticity modulus values was statistically significant.

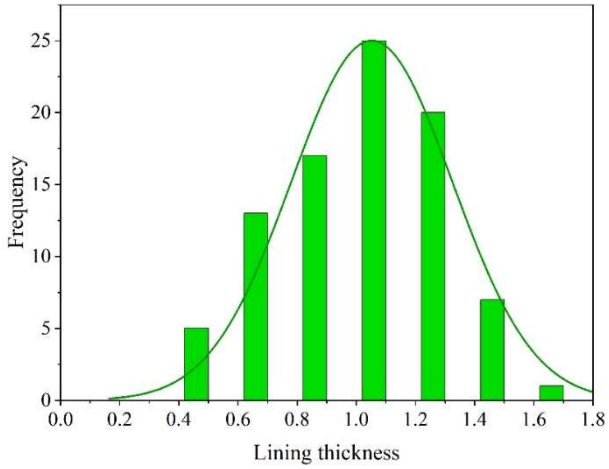

Figure 1: Frequency distribution of endometrial thickness in PCOS group

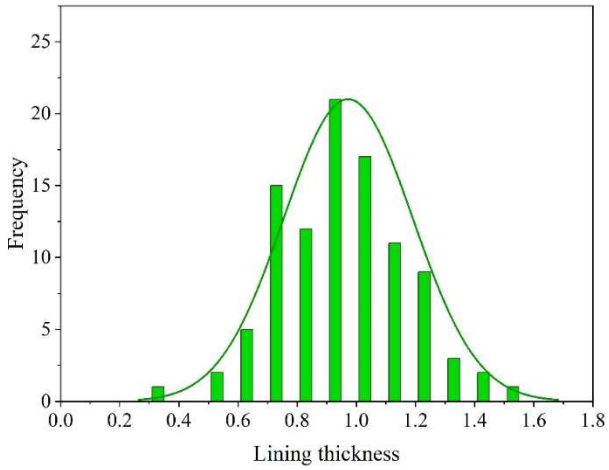

Figure 2: Frequency distribution of endometrial thickness in the control group

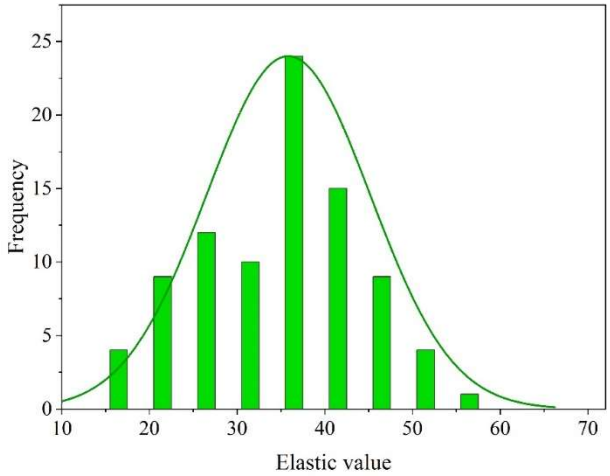

Figure 3: Frequency distribution of endometrial elasticity values in pcos group

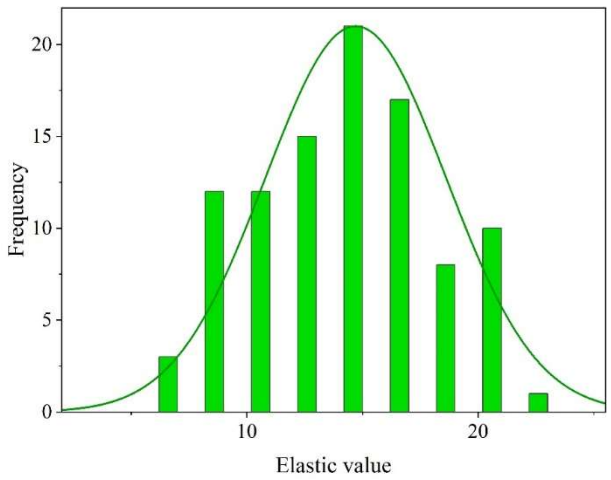

Figure 4: Frequency distribution of endometrial elasticity values in the control group

III. C. Comparison of multimodal ultrasonography scores

The results of multimodal ultrasonography score comparison are shown in Table 2. The endometrial thickness score, VFI index score and total score of multimodal ultrasonography in the observation group were lower than those in the control group, P<0.05; there was no significant difference in other scores compared with those in the control group, P>0.05.

Table 2: Comparison of multimodal ultrasonic examination scores($\bar{x} \pm s$)

Index	Control group	Case group	t	P
Endometrial grade	21.57±1.42	21.19±1.45	1.173	0.264
Endometrial thickness rating	21.79±1.73	21.57±1.61	3.291	0.005
Endometrial blood flow grading	21.89±1.52	21.73±1.43	1.601	0.124
endometriosis	22.31±1.44	22.19±1.32	1.584	0.127
EV score	22.29±1.63	22.19±1.58	1.462	0.154
VFI index score	22.47±1.67	22.08±1.59	3.235	0.005
Multimodal ultrasonic check score	31.49±2.82	28.79±2.94	2.618	0.014

III. D. Correlation analysis between ultrasound parameters and VEGF expression levels

The scatter of correlation between endometrial blood flow VI, FI, VFI and endometrial VEGF mRNA is shown in Figures 5 to 6. Endometrial blood flow VI, FI, VFI and endometrial VEGF mRNA expression level in the “implantation window” period had a certain linear relationship, while uterine spiral artery RI, PI and endometrial volume showed a scattered distribution with endometrial VEGF mRNA expression level.

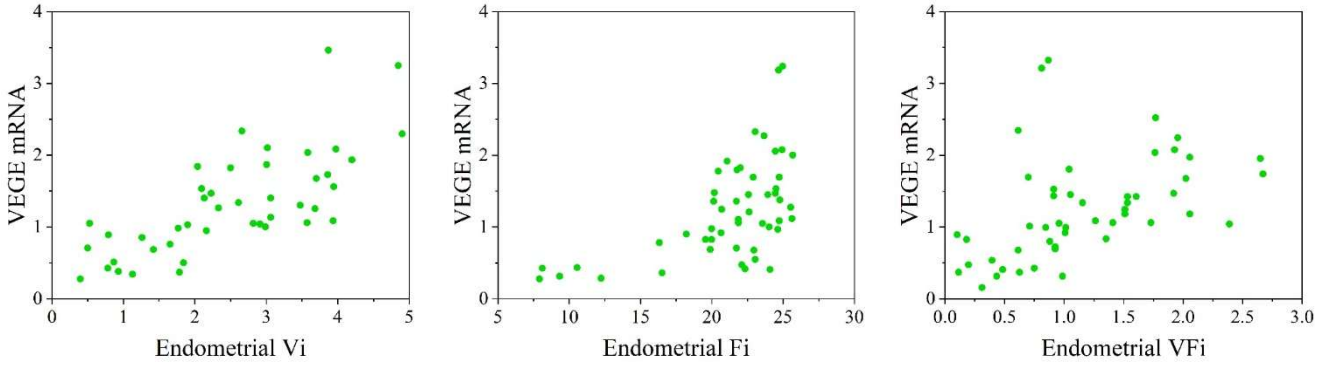

(a) Endometrium Vi (b) Endometrium Fi (c) Endometrial VFi

Figure 5: Correlation between endometrial blood flow Vi, Fi, VFi and endometrial vegf mrna

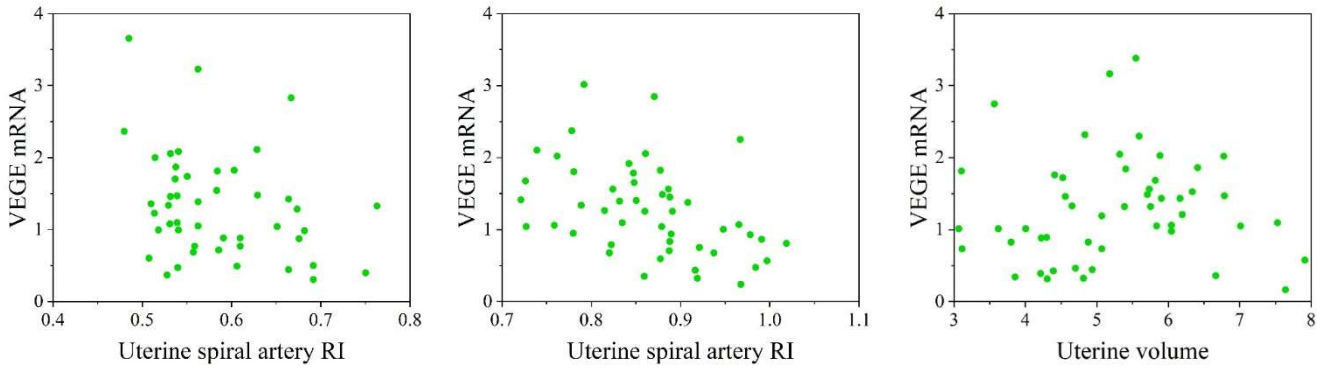

(a) Uterine spiral artery RI (b) Uterine spiral artery PI (c) Uterine volume

Figure 6: Scatter diagram of correlation between spiral artery RI, p and endometrial vegf mrna

According to the method of Pearson analysis [19], the correlation between endometrial VEGF expression and endometrial ultrasound data was analyzed, and the results are shown in Table 3. There was a significant positive correlation between endometrial VEGF mRNA expression level and endometrial blood flow VI in the “implantation window” period (r=0.744, P<0.01); and a moderate positive correlation with endometrial blood flow FI and VFI (r=0.522, P<0.01; r=0.435, P=0.001).

Table 3: Correlation between endometrial VEGF expression and endometrial ultrasound data

Variable 1	Variable 2	Correlation coefficient r	Pvalue
Endometrial vegf mrna	Endometrial vegf protein	0.895	<0.001
Endometrial vegf mrna	Endometrial angiography VI	0.744	<0.001
Endometrial vegf mrna	Endometrial blood flow index	0.522	<0.001
Endometrial vegf mrna	Endometrial vascularization VFI	0.435	0.001

III. E. Comparison of sensitivity in predicting IVF-ET pregnancy outcomes

The ROC curves of endometrium-related indexes are shown in Figure 7, and the area under the ROC curves of endometrial indexes in the "implant window" period is as follows: endometrial blood flow VI> endometrial volume> spiral artery RI>spiral artery PI> endometrial blood flow FI>VEGF mRNA amplification fold>VEGF protein gray > endometrial blood flow VFI (i.e., 0.951>0.890> 0.829>0.828>0.791>0.763> 0.743>0.718).

The ROC curves showed that the above endometrial indicators during the “implantation window” period, i.e. endometrial blood flow VI, FI and VFI, endometrial volume, spiral artery RI and PI, as well as the endometrial VEGF mRAN and protein expression levels, were predictive of pregnancy outcome (P < 0.01).

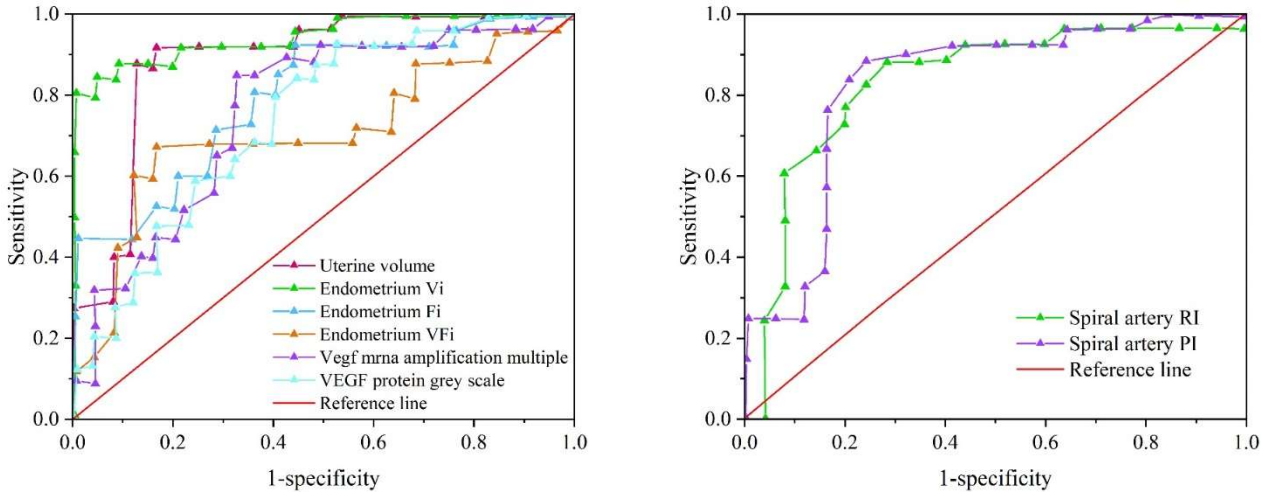

(a) Curve 1 (b) Curve 2

Figure 7: The ROC curve of endometrial related indicators

A comparison of the sensitivity of various endometrial-related indicators to predict IVF-ET pregnancy outcome is shown in Table 4. Meanwhile, the sensitivity of endometrial blood flow VFI was relatively weak (69%) and the specificity of endometrial VEGF protein expression level was relatively poor (49%) among all indicators. The area under the ROC curve for endothelial blood flow VI was the largest among the above indicators, with a sensitivity of 90% and a specificity of 94% when VI had an intercept value of 2.472.

Table 4: Comparison of the sensitivity of various endometrial related indicators to pregnancy outcome

Correlation index	Undercurve product	P value	Critical point	Sensitivity(%)	Specificity(%)
Endometrial volume	0.878	<0.001	4.953	94	85
Endometrial angiography vi	0.953	<0.001	2.472	90	94
Endometrial blood flow index	0.782	<0.001	21.875	94	58
Endometrial vascularization vfi	0.723	0.007	1.145	71	85
Spiral artery ri	0.834	<0.001	0.672	90	75
Spiral artery PI	0.829	<0.001	0.891	90	79
Vegf mrna amplification multiple	0.767	0.001	1.024	85	71
Vegf protein grey scale	0.739	0.002	0.331	94	50

IV. Discussion

When the difference in overall endometrial thickness between the PCOS group and the control group ($P > 0.05$) had not yet reflected the changes in ER between the two groups, the difference in endometrial elastic modulus values between the two groups ($P < 0.05$) showed that the endometrial stiffness of the PCOS group was significantly higher than that of the control group, which showed that the endometrial thickness could not reflect changes in ER during the menstrual cycle in real time, which was consistent with most of the views that the ultrasound index of uterine thickness could not be used purely as an This is consistent with the majority view that the uterine thickness ultrasound index alone cannot be used as a criterion for evaluating ER. Some scholars have used three-dimensional ultrasound to measure endometrial volume, which is more reflective of the overall endometrial condition than endometrial thickness alone, and have suggested that excess body mass index may lead to a decrease in endometrial volume and thus lower ER. However, there is a lack of evidence to support the correlation between the change in endometrial volume and ER, and the endometrial volume changes with the progression of the pregnancy.

The endometrial thickness score, VFI index score and total multimodal ultrasonography score were observed to be lower than those of the control group ($P<0.05$), and the endometrial thickness, endometrial vascular hemodynamic parameters, and endometrial status of the unfertilized women were significantly lower than those of the successfully fertilized women, and the multimodal ultrasonography score has a higher value in assessing endometrial tolerance in women who are ready to conceive.

Scatterplot analysis in this study showed that uterine spiral artery RI and PI, endometrial volume and endometrial VEGF mRNA expression level were scattered and did not correlate with each other in a convergent manner; however, there was a linear relationship between endometrial blood flow VI, FI, and VFI and VEGF mRNA expression level. Using Pearson correlation coefficient analysis, the correlation coefficients of endometrial blood flow VI, FI, VFI and endometrial VEGF mRNA were $r=0.744$, 0.522, 0.435, with P values <0.05. It can be seen that endometrial ultrasonographic blood flow parameters VI, FI, and VFI in the luteal phase are positively correlated with the expression level of endometrial VEGF, and endometrial blood flow VI had a highly positive correlation with endothelial VEGF expression level. We speculate that although the main role of endothelial VEGF is to promote endothelial neovascularization, the regulatory mechanism of endothelial angiogenesis includes many other pathways, such as integrins, hypoxia-producing factors, estrogen and progesterone, etc. Therefore, VI, FI, and VFI, which reflect the overall situation of endothelial blood flow in ultrasonography, correlate strongly with the expression level of VEGF, whereas helical arterial RI and PI do not have any significant correlation with it.

V. Conclusion

In this study, we compared the differences in endometrial-related indicators between the PCOS group and the control group. The results showed that the difference between the PCOS group and the control group in terms of endometrial thickness was not significant ($P > 0.05$), but in terms of endometrial elastic modulus, the PCOS group was significantly higher than the control group, and the difference was statistically significant ($P < 0.05$). In addition, endometrial blood flow parameters VI, FI, VFI and endometrial VEGF expression level showed significant positive correlation. The strongest correlation was found between endometrial blood flow VI and VEGF expression level, with a correlation coefficient of 0.744 ($P < 0.01$), which suggests that endometrial blood flow VI may become a key

indicator for assessing endometrial tolerance. By further analysis, we found that endometrial blood flow VI had the largest area under the ROC curve (0.953), with a sensitivity of 90% and a specificity of 94%. These results suggest that 3D ultrasound technology combined with hemodynamic parameters can effectively assess endometrial tolerance and provide strong support for pregnancy outcome prediction in assisted reproduction. This method not only improves the accuracy of tolerance assessment, but also provides a more reliable basis for clinical decision-making.

References

[1] Lessey, B. A., & Young, S. L. (2019). What exactly is endometrial receptivity?. Fertility and sterility, 111(4), 611-617.

[2] Li, Y., Li, Q., Chen, D., Mao, W., & Zhang, Y. (2024). Recent advances in understanding the role of uterine microbiota in endometrial receptivity and its impact on embryo implantation failure. Cellular and Molecular Biology, 70(10), 110-116.

[3] Neykova, K., Tosto, V., Giardina, I., Tsibizova, V., & Vakrilov, G. (2022). Endometrial receptivity and pregnancy outcome. The Journal of Maternal-Fetal & Neonatal Medicine, 35(13), 2591-2605.

[4] Craciunas, L., Pickering, O., Chu, J., Choudhary, M., Žurauskienė, J., & Coomarasamy, A. (2021). The transcriptomic profile of endometrial receptivity in recurrent miscarriage. European Journal of Obstetrics & Gynecology and Reproductive Biology, 261, 211-216.

[5] Coughlan, C. (2018). What to do when good-quality embryos repeatedly fail to implant. Best Practice & Research Clinical Obstetrics & Gynaecology, 53, 48-59.

[6] Xu, S., Diao, H., Xiong, Y., Zhang, C., Zhang, Y., & Zhang, Y. (2025). The study on the clinical efficacy of endometrial receptivity analysis and influence factors of displaced window of implantation. Scientific Reports, 15(1), 7326.

[7] Zhang, C. H., Chen, C., Wang, J. R., Wang, Y., Wen, S. X., Cao, Y. P., & Qian, W. P. (2022). An endometrial receptivity scoring system basing on the endometrial thickness, volume, echo, peristalsis, and blood flow evaluated by ultrasonography. Frontiers in endocrinology, 13, 907874.

[8] Cheng, F., Xv, B. M., Liu, Y. L., Sun, R., Wang, L., & Yi, J. L. (2022). Endometrial microstimulation effects on endometrial receptivity assessed by transvaginal color Doppler sonography. BMC Women's Health, 22(1), 508.

[9] Li, M., Zhu, X., Wang, L., Fu, H., Zhao, W., Zhou, C., ... & Yao, B. (2024). Evaluation of endometrial receptivity by ultrasound elastography to predict pregnancy outcome is a non-invasive and worthwhile method. Biotechnology and Genetic Engineering Reviews, 40(1), 284-298.

[10] Jiao, Y., Xue, N., Shui, X., Yu, C., & Hu, C. (2020). Application of ultrasound multimodal score in the assessment of endometrial receptivity in patients with artificial abortion. Insights into imaging, 11, 1-7.

[11] Wu, J., Sheng, J., Wu, X., & Wu, Q. (2023). Ultrasound assessed endometrial receptivity measures for the prediction of in vitro fertilization embryo transfer clinical pregnancy outcomes: A meta analysis and systematic review. Experimental and Therapeutic Medicine, 26(3), 453.

[12] Li, X., Peng, Y., Mao, Y., Li, Y., Gong, F., & Ouyang, Y. (2023). Endometrial receptivity change: ultrasound evaluation on ovulation day and transplantation day during the natural frozen embryo transfer cycle. Frontiers in Endocrinology, 14, 1118044.

[13] Haas, J., & Casper, R. F. (2022). Observations on clinical assessment of endometrial receptivity. Fertility and sterility, 118(5), 828-831.

[14] Liu, Z., Liu, Y., Liu, J., Sun, H., Liu, J., Hou, C., ... & Li, B. (2024). Noninvasive and fast method of calculation for instantaneous wave-free ratio based on haemodynamics and deep learning. Computer Methods and Programs in Biomedicine, 255, 108355.

[15] Zhou, Z., Wang, Y., Guo, Y., Qi, Y., & Yu, J. (2019). Image quality improvement of hand-held ultrasound devices with a two-stage generative adversarial network. IEEE Transactions on Biomedical Engineering, 67(1), 298-311.

[16] Wang, X., Bao, N., Xin, X., Tan, J., Li, H., Zhou, S., & Liu, H. (2022). Automatic evaluation of endometrial receptivity in three-dimensional transvaginal ultrasound images based on 3D U-Net segmentation. Quantitative Imaging in Medicine and Surgery, 12(8), 4095.

[17] Fadhil Abbas Fadhil,Farah Tawfiq Abdul Hussien Alhilo & Mohammed T. Abdulhadi. (2024). Enhancing data security using Laplacian of Gaussian and Chacha20 encryption algorithm. Journal of Intelligent Systems,33(1),

[18] Yiyun Gan,Linyu Huang,Qian Ning,Yong Guo & Yongsheng Li. (2025). Enhanced detection of measurement anomalies in cartridge cases using 3D gray-level co-occurrence matrix. . Forensic science international,367,112366.

[19] Zhongfeng Pan,Daming Xu,Yibo Zhang,Minzhen Wang,Zhuang Wang,Jiang Yu & Guangxin Zhang. (2024). New energy transmission line fault location method based on Pearson correlation coefficient. Journal of Physics: Conference Series,2717(1),